

NON-ISOTHERMAL HEATING OF MATRIX BLOCKS UNDER CONSTANT HEAT FLUX

CALENTAMIENTO NO-ISOTÉRMICO DE BLOQUES MATRICIALES BAJO UN FLUX CONSTANTE DE CALOR

R.G. Suarez-Suarez^{1*}, S.H. Hejazi², C.E. Scott²

¹*Tecnologico de Monterrey. Av de los Poetas 100, Santa Fe, 01389, CDMX, México.*

²*University of Calgary. 2500 University Dr NW, Calgary, AB T2N 1N4, Canada.*

Received: October 2, 2018; Accepted: January 14, 2019

Abstract

Nanocatalytic *in-situ* upgrading is a novel enhanced oil recovery process that consists of injecting ultra-dispersed nanocatalyst into a preheated oil reservoir. Nanocatalyst propagates into the porous medium and promotes exothermic reactions that provide additional heating to the reservoir. The objective of this work is to capture the main thermal processes involved in nanocatalytic *in-situ* upgrading by presenting a simple analytical model. This model considers the transient temperature distribution within a matrix block heated by a constant temperature and heat flux. To achieve this goal, the formulation of various stages including heating up, hydroprocessing heating, and post-hydroprocessing heating were carried out based on an energy balance equation, various boundary conditions and using a semi-analytical method known as Heat Integral Method (HIM) to solve the equation. This work provides simple analytical solutions for modeling the nanocatalytic *in-situ* process. Hence, it can be used for scale-up of heavy oil recovery from large matrix blocks of naturally-fractured-carbonate reservoirs.

Keywords: *in-situ* upgrading, Heat Integral Method (HIM), enhanced oil recovery, heavy oil, naturally-fractured-carbonate reservoirs.

Resumen

El mejoramiento de crudo pesado en sitio es un proceso novedoso de recuperación mejorada que consiste en inyectar nanocatalizador ultra-disperso en un yacimiento precalentado. El nanocatalizador se propaga en el medio poroso y promueve reacciones exotérmicas que proveen calentamiento adicional al yacimiento. El objetivo de este trabajo es capturar los principales procesos térmicos involucrados en el proceso de mejoramiento de crudo pesado en sitio presentando un modelo analítico simple. El modelo considera la distribución de temperatura transitoria en un bloque matricial calentado por temperatura y un flux de calor constante. En el modelo varias etapas del calentamiento del yacimiento fueron formuladas, incluyendo, calentamiento inicial, calentamiento por hidroprocesamiento, y calentamiento después del hidroprocesamiento; para ello la ecuación de balance de energía se resolvió utilizando varias condiciones a la frontera y un método semi-analítico conocido como Heat Integral Method. Este trabajo provee soluciones analíticas simples para modelar el proceso de mejoramiento de crudo pesado en sitio, y así calcular el recobro de aceite pesado de largos bloques matriciales en yacimientos carbonatados naturalmente fracturados.

Palabras clave: mejoramiento de crudo pesado en sitio, Heat Integral Method (HIM), recuperación mejorada, aceite pesado, yacimientos carbonatados naturalmente fracturados.

1 Introduction

Oil production from heavy-oil-fractured reservoirs usually requires assistance of an enhanced oil recovery technique (Babadagli, *et al.*, 2008; Ferno, 2012). Most heavy-oil fractured reservoirs are oil wet; therefore, water injection may not lead to a significant

improvement in oil recovery. Viscosity reduction by miscible, thermal and chemical processes has potential to increase flow rates in heavy-oil-fractured reservoirs (Babadagli, 2003). However, the success of any miscible, thermal and chemical process highly depends on the heat and mass transfer of the injected agent in the porous media.

* Corresponding author. E-mail: ricardosuarezsuarez88@gmail.com

<https://doi.org/10.24275/uam/izt/dcbi/revmexingquim/2019v18n3/SuarezS>

issn-e: 2395-8472

In thermal processes, steam is usually the agent injected into the fracture networks to create a thermal zone and to produce the oil contained in the fractures. Thus, the primary objective is to reduce the viscosity of the oil contained in matrix blocks (Pooladi-Darvish, *et al.*, 1994; van Heel, *et al.*, 2008). Steam injection in heavy-oil-fractures reservoirs has been widely proposed and studied (Nolan, *et al.*, 1980; van Wunnik, *et al.*, 1992; Mollaei, *et al.*, 2007; Verlaan, *et al.*, 2008; Souraki, *et al.*, 2011; van Heel, *et al.*, 2008). However, its use may not be effective in reservoirs where water availability is scarce and heat losses are considerable because of large matrix blocks in deep formations (Babadagli, *et al.*, 2008). Therefore, new technologies like hot solvent-assisted oil recovery, *in-situ* combustion and *in-situ* upgrading are proposed to recover oil from fractured reservoirs (Sherratt *et al.*, 2018; Norasyikin *et al.*, 2016; Pereira-Almao 2012). These techniques reduce oil viscosity by thermal and mass diffusivities and consequently upgrading the oil inside the reservoir. In particular, *in-situ* upgrading of heavy oil by catalytic hydrogenation is a process in which a hot stream of fluids with ultra-dispersed nanocatalyst is injected directly into the reservoir instead of using such nanocatalyst in a refinery (Huirache-Acuña, *et al.*, 2010). The aim is to heat the reservoir until it reaches sufficiently high temperatures to produce reasonable upgrading and propagate the nano-catalyst over long distances inside the reservoir. The *in-situ* upgrading technology can heat the matrix blocks in two ways: by injecting a hot fluid into the formation and/or by the nano-dispersed catalyst that promotes exothermic reactions. The *in-situ* upgrading process is transient in nature. Thus, the transport equations are described by nonlinear partial differential equations. The solution of these equations requires large computational time and it depends on chemical kinetic models and parameters of the involved chemical reactions. Therefore, a simple model to describe the *in-situ* upgrading process is desirable for practical purposes. Heat transportation in reservoirs have been studied previously (Pooladi-Darvish, *et al.*, 1994; Martínez-Médez E., *et al.*, 2006; Olea-Gonzalez U., *et al.*, 2007; van Heel, *et al.*, 2008; Haseli, *et al.*, 2012). However, none of these works considered heat flux, condition that is of importance for chemical-enhanced-recovery processes. In this work, we developed a simple mathematical model and obtain analytical solutions to represent the heat transfer component of the nanocatalytic *in-situ* upgrading process.

We obtained the temperature profiles at various modes of heating inside a 1D matrix block. Consequently, oil recovery due to thermal expansion is estimated.

2 Description of the process

Nanocatalyst *in-situ* upgrading is an enhanced oil recovery process in which energy is applied for upgrading and incrementing the recovery factor of heavy oil reservoirs. Therefore, this novel technology combines thermal oil recovery processes and *in-situ* nanocatalytic hydrogenation (Pereira-Almao, 2012). A successful upgrading process needs heating up the reservoir while the nanocatalyst is introduced. Coy (2013) demonstrated that vacuum residue, the bottom product from the vacuum distillation unit, can meet both requirements: heat the matrix and carry the nanocatalyst in the porous media. Moreover, the use of vacuum residue has advantages for deep-high-pressure reservoirs, where the use of steam is not feasible.

During nanocatalytic *in-situ* upgrading, the reservoir is first heated using hot vacuum residue until the temperature of the reaction is achieved. Then, the reservoir starts to work as a reactor. Rendon (2011) and Galarraga (2011) conducted thermodynamic spontaneity evaluations to prove that chemical reactions occur at a temperature range of 320 to 380°C. Most reactions associated with hydroprocessing of vacuum residue and oil contained in the reservoir are exothermic (Elahi, *et al.*, 2018). Thus, additional thermal energy is transferred from the fracture to the matrix block. Exothermic reactions will increase the fracture temperature up to a maximum value where residue conversion reaches to an equilibrium. After this point, it is assumed that the rate of heat loss from fracture to matrix equals the rate of heat generation by the reactions. Thus, the temperature in the fractures remains constant.

Thus, three stages can be identified in a reservoir heated by nanocatalytic *in-situ* process:

1. **Initial heating up:** oil in the fractures is mobilized and the matrix block is heated by a constant temperature provided by the hot vacuum residue.
2. **Hydroprocessing heating:** the reservoir works as a chemical reactor. Matrix blocks are heated by a constant heat flux generated from the exothermic chemical reactions.

3. **Post-hydroprocessing heating:** residue conversion reaches to an equilibrium and the temperature in the fractures remains constant.

3 Mathematical formulation

This section describes the physical system and assumptions used to develop the model. Figure 1 depicts the matrix block, represented by a vertical slab, heated from its adjacent fractures filled with vacuum residue. There is no heat flow from the top and bottom boundary of the slab. Therefore, for this homogeneous and isotropic matrix block, the energy balance is reduced to a 1D transient heat conduction equation.

$$\frac{\partial T}{\partial t} = \alpha \frac{\partial^2 T}{\partial x^2} \quad (1)$$

Equation 1 assumes that there is no heat transfer by convection in the system if small fluid velocities are considered.

We also assume a constant thermal diffusion coefficient for the porous medium, existence of thermodynamic equilibrium and uniform initial temperature T_r for the matrix block according to previous studies (Pooladi-Darvish, *et al.*, 1994; van Heel, *et al.*, 2008; Haseli, *et al.*, 2012). Because of symmetry, we only consider half of the matrix block and $x = L_m$ represents the middle cross section of slab where there is a zero heat flux. In the following section, we use **Equation 1** with the appropriate boundary and initial conditions to model the three stages of reservoir heating previously mentioned.

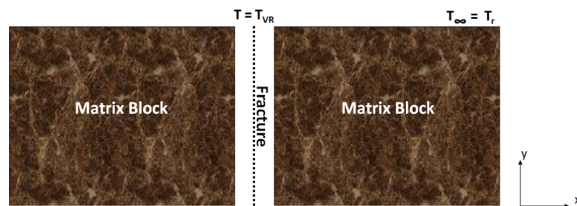


Fig. 1. Schematic representation of the physical problem.

3.1 Stage 1: Initial heating up

Initial heating of matrix block involves injection of hot vacuum residue at a constant temperature. This stage may result in two different heating regimes: an

infinite acting regime and a finite acting regime. In the first one, the heat propagation has not reached to the symmetry boundary at $x = L_m$ and in the latter the temperature at $x = L_m$ starts to increase. The end of initial heating stage and start of hydroprocessing stage depends on the slab size and the required temperature for the reaction initiation. However, it is assumed that the reaction starts almost right after the introduction of hot vacuum residue. Therefore, the initial heating process corresponds to an infinite acting regime. **Equations 2-4** present the initial and boundary conditions for this stage:

$$T(t = 0, x \geq 0) = T_r \quad (2)$$

$$T(t \geq 0, x = 0) = T_{VR} \quad (3)$$

$$T(t \geq 0, x = L_m) = T_r \quad (4)$$

All equations are expressed in dimensionless form using the following definitions for dimensionless temperature, length and time:

$$T_D = \frac{T - T_r}{T_{VR} - T_r} \quad (5)$$

$$x_D = \frac{x}{L_m} \quad (6)$$

$$t_D = \frac{t}{\frac{L_m^2}{\alpha}} \quad (7)$$

We also defined characteristic time and length scales, $\tau = L_m^2/\alpha$ and $l = L_m$, respectively. Thus, the dimensionless form of the heat equation and its initial and boundary conditions are:

$$\frac{\partial T_D}{\partial t_D} = \frac{\partial^2 T_D}{\partial x_D^2} \quad (8)$$

$$T_D(t_D = 0, x_D \geq 0) = 0 \quad (9)$$

$$T_D(t_D \geq 0, x_D = 0) = 1 \quad (10)$$

$$T_D(t_D \geq 0, x_D = 1) = 0 \quad (11)$$

For the infinite acting regime, we can solve the above partial differential equation using Laplace transform which results in the following solution:

$$T_D = \operatorname{erfc}\left(\frac{x_D}{2\sqrt{t_D}}\right) \quad (12)$$

This solution has been presented by (Pooladi-Darvish, *et al.*, 1994; van Heel, *et al.*, 2008). Moreover, Pooladi-Darvish *et al.* (1994) solved the

system of Equations 9-12 using Heat Integral Method (HIM) technique. The HIM is a powerful approach that provides approximate analytical solutions to diffusion problems (Goodman, 1964). Considering a third order polynomial for the temperature distribution, the HIM solution can be found as:

$$T_D = \left(1 - \frac{x_D}{\sqrt{24t_D}}\right)^3 \quad (13)$$

The derivation of this solution is provided by Pooladi-Darvish *et al.* (1994) and also in Appendix A. Furthermore, Pooladi-Darvish *et al.* (1994) verified that this solution can accurately predict the temperature distribution in a single block slab. Also, it was demonstrated that the HIM solutions can be easily used for evaluating oil recovery. Therefore, we later use the HIM solution to calculate oil production at each heating stages.

Equation 13 provides the unsteady-state temperature profiles in the semi-infinite matrix block heated by a constant temperature. As discussed earlier, we assumed that the initial heating stage only involves the infinite acting regime. Thus, this process ends once the heat wave reaches to the symmetry boundary. We can find this time when the heat penetration depth (δ in the Appendix A) is equal to one. Therefore:

$$t_{D1} = \frac{1}{24} \quad (14)$$

t_{D1} denotes the end of the initial heating-up process and the start of hydroprocessing heating process in which additional energy generated by exothermic reactions is transferred to the matrix block.

3.2 Stage 2: Hydroprocessing heating

After initial heating, additional energy is provided to the surface of the matrix block by exothermic reactions. This flow of energy has to be taken into account to represent nanocatalytic *in-situ* upgrading. Hence, we used the HIM technique to solve the 1D heat conduction equation with the following boundary and initial conditions.

$$T_D = T_{D,1} \text{ at } t_{D1} \quad (15)$$

$$\frac{\partial T_D}{\partial x_D} \Big|_{x_D=0} = q_D \quad (16)$$

$$\frac{\partial T_D}{\partial x_D} \Big|_{x_D=1} = 0 \quad (17)$$

where q_D is the constant dimensionless heat flux given by:

$$q_D = \frac{qL_m}{k(T_{VR} - T_r)} \quad (18)$$

For a known oil and reaction temperature (T_{reac}) the heat flux is described as:

$$q = h(T_{reac} - T_{VR}) + \sigma \epsilon (T_{reac}^4 - T_{VR}^4) \quad (19)$$

Solution of the heat conduction equation with the specified boundary condition is pseudo-steady state. Using a third order polynomial and the HIM technique, the temperature distribution during the hydroprocessing stage can be found as:

$$T_{Dh} = 1 + q_D \left(t_D - \frac{1}{24}\right) - q_D x_D + (2q_D - 3)x_D^2 + (2 - q_D)x_D^3 \quad (20)$$

Details on the derivation of this solution are provided in Appendix B. This solution represents the unsteady-state temperature profile of a semi-infinite matrix block heated by a constant heat flux. This additional heat is provided by the exothermic reactions that take place in the reservoir while the vacuum residue and the oil in place react with hydrogen in the presence of the nano-catalyst. Hassazadeh, *et al.* (2010) model the kinetics parameters of ultra-dispersed *in-situ* catalytic upgrading experiments performed in a batch reactor. They scale the reaction time with $t_{Dreac} = t\tau_1$ where $\tau_1 = 1/k_g$, and k_g is the global reaction constant. Results from Hassazadeh *et al.* (2010) demonstrate that for practical applications of nanocatalytic *in-situ* upgrading, it is valid to assume that residue conversion happens at small residence times, i.e. $t_{Dreac} < 1$. Therefore, we assumed that the hydroprocessing stage ends at:

$$t_{Dh} = t_{D1} + \frac{\tau_1}{\tau} t_{Dreac} \quad (21)$$

3.3 Stage 3: Post-hydroprocessing heating

After completion of hydroprocessing, the temperature in the fractures reaches to a maximum value and becomes plateau as the vacuum residue conversion reaches to an equilibrium. The boundary conditions for this stage are presented as:

$$T_{D1} = T_{Dh}(x_D = 0, t_d = t_{Dh}) \quad (22)$$

$$T_{D1} = T_{D2} \text{ at } x_D = \frac{1}{2} \quad (23)$$

$$\frac{\partial T_{D2}}{\partial x_D} \Big|_{x_D=1} = 0 \tag{24}$$

$$\frac{\partial T_{D2}}{\partial x_D} \Big|_{x_D=1/2} = \frac{\partial T_{D1}}{\partial x_D} \Big|_{x_D=1/2} \tag{25}$$

The heat conduction equation is solved with the above boundary conditions using the HIM. The domain of interest was divided into two sections ($0 \leq x_D \leq 1/2$ and $1/2 \leq x_D \leq 1$), where the temperature profiles for each section are obtained as:

$$T_{D1} = T_{Dh}(0, t_{Dh}) + b(t_D)x_D + c(t_D)x_D^2 \quad x_D \in [0, 1/2] \tag{26}$$

$$T_{D2} = T_{Dh}(0, t_{Dh}) + b(t_D)\left(-\frac{1}{4} + 2x_D - x_D^2\right) + c(t_D)\left(-\frac{1}{2} + 2x_D - x_D^2\right) \quad x_D \in [0, 1] \tag{27}$$

Details on the solution and $b(t_D)$ and $c(t_D)$ coefficients are presented in Appendix C.

4 Results and discussion

The mathematical solutions presented in the previous section capture the main characteristics of heating a matrix block by nanocatalytic *in-situ* upgrading. The temperature evolution of a single block heated by nano-catalytic *in-situ* upgrading for various stages of heating is presented in Figure 2, Figure 3, and Figure 4.

Figure 2 shows that during the early stage, the matrix block is heated by a constant temperature until the heat wave reaches the symmetry boundary. This is similar to heating the matrix block with steam.

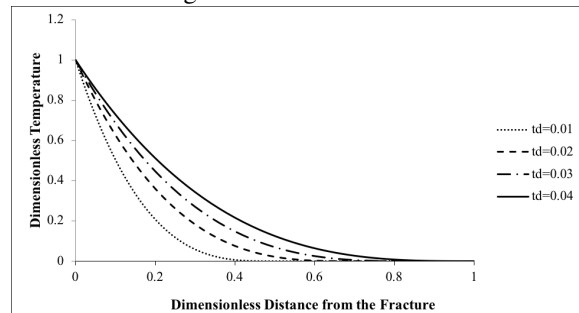


Fig. 2. Initial heating up of a single matrix block.

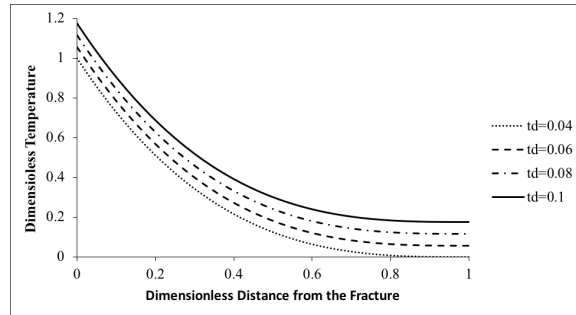


Fig. 3. Hydroprocessing heating of a single matrix block.

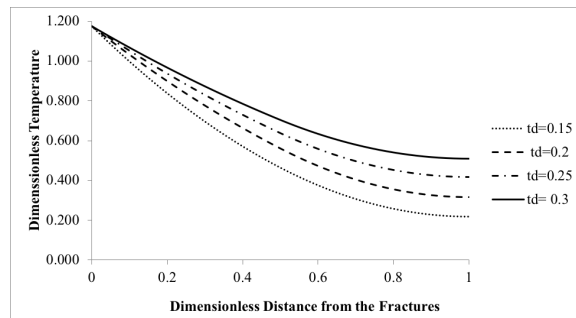


Fig. 4. Post-hydroprocessing heating of a single matrix block.

Figure 3 shows that after reaching the symmetry boundary, the temperature starts to rise. Temperature rises because at this point a constant flow of energy, generated from exothermic reactions, increases the temperature in the system. From this figure we can note that not only the gradient is increasing in time at an equal rate everywhere but also there is a fixed-shape temperature profile in the block. Therefore, by representing the hydroprocessing heating stage, we have developed a pseudo-steady state temperature solution that has not been previously presented in the literature. Moreover, this solution can be of great interests to represent other thermal processes such as electrical heating (Lashgari et al., 2016).

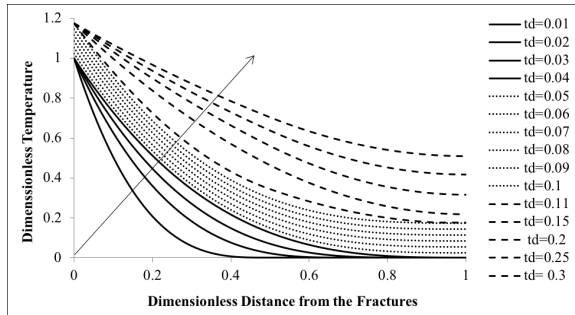


Fig. 5. Nanocatalytic *in-situ* upgrading heating up process of a single matrix block.

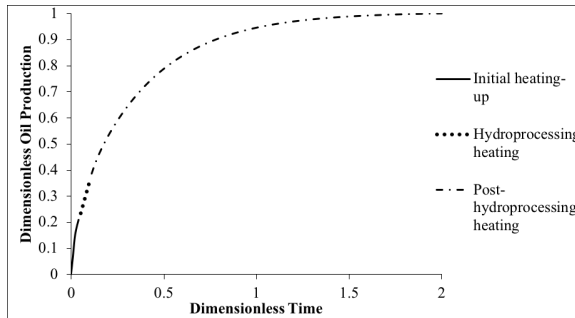


Fig. 6. Dimensionless cumulative oil production from a single matrix block due to thermal expansion.

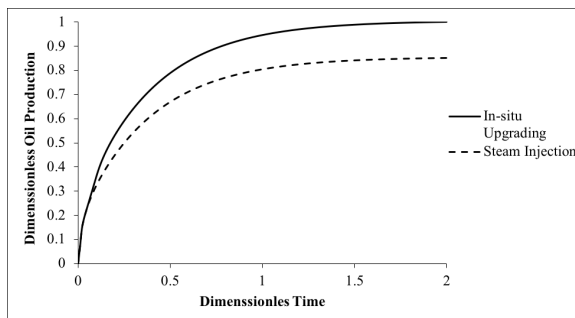


Fig. 7. Cumulative oil production from a matrix block due to thermal expansion.

From Figure 4, we can observe that after hydroprocessing heating the temperature in the fracture does not increase anymore. Therefore, at this point the matrix block is heated by a constant temperature. During this stage the heat wave has reached to the symmetry boundary; thus, the temperature at the center rises until thermal equilibrium is achieved.

Figure 5 shows early and late-time temperature distribution, which includes the various stages of heating during nano-catalytic *in-situ* upgrading. Having the temperature distribution, we can evaluate

the cumulative oil production by nanocatalytic *in-situ* upgrading process.

$$Q_0(t_D) = C_{1D} \int_0^{x_D} (T_D) dx_D \quad (28)$$

$$C_{1D} = \frac{\varphi W H L_m (S_0 \delta \beta_{0p} - S_{wc} \delta \beta_{wp}) (T_{VR} - T_R)}{B_0} \quad (29)$$

$$Q_{0D} = \frac{Q_0}{Q_{0T}} \quad (30)$$

Equation 28 and 29 are suggested by (van Heel, et al., 2008) for calculating the cumulative oil production by thermal expansion. Using the temperature profiles, Equation 28 can be integrated to obtain cumulative oil production as:

$$Q_{0D}(t_D) = \int_0^1 \left(\left(1 - \frac{x_D}{\sqrt{24t_D}} \right)^3 \right) dx_D \quad t_D \leq t_{D1} \quad (31)$$

$$Q_{0D}(t_D) = \int_0^1 \left(1 + q_D \left(t_D - \frac{1}{24} \right) - q_D x_D + (2q_D - 3)x_D^2 + (2 - q_D)x_D^3 \right) dx_D \quad t_{D1} \leq t_D \leq t_{Dh} \quad (32)$$

$$Q_{0D}(t_D) = \int_0^{\frac{1}{2}} (T_{Dh}(0, t_{Dh}) + b(t_D)x_D + c(t_D)x_D^2) dx_D \quad t_{D2} > t_{Dh} \quad (33)$$

$$Q_{0D}(t_D) = \int_{\frac{1}{2}}^1 \left(T_{Dh}(0, t_{Dh}) + b(t_D) \left(-\frac{1}{4} + 2x_D - x_D^2 \right) + c(t_D) \left(-\frac{1}{2} + 2x_D - x_D^2 \right) \right) dx_D \quad t_{D2} > t_{Dh} \quad (34)$$

Figure 6 shows the cumulative oil production under the three different thermal stages of nanocatalytic *in-situ* upgrading. Moreover, for comparison purposes, we evaluated the oil recovery of the same matrix block when it is only heated at constant temperature, i.e. steam heating. Figure 7 shows cumulative oil production from a single block due to thermal expansion for both nanocatalytic *in-situ* upgrading (constant temperature and heat flux) and steaming (constant temperature). The graph shows

that we get an incremental oil recovery through thermal expansion when applying nanocatalytic *in-situ* upgrading, a hybrid chemical and thermal enhanced oil recovery.

Conclusions

We developed a simple analytical model to represent the thermal behavior of the nano-catalytic *in-situ* upgrading process inside a reservoir. This model introduced the formulation of nanocatalytic *in-situ* upgrading stages in which the reservoir was heated by a constant temperature and heat flux. The different stages were described by unsteady state heat conduction equation which was converted, by means of space integration, into ordinary differential equations. The resultant solutions were in the form of simple algebraic expressions. Algebraic solutions are useful since they can be easily integrated or coupled with flow equations or equations of state. Temperature profiles for the various stages of process were obtained. It was interesting to report a pseudo-steady state temperature distribution in the matrix block once we had the constant heat flux resulted from the exothermic reaction. Oil recovery resulted from thermal expansion was evaluated. The model demonstrated that nanocatalytic *in-situ* upgrading could yield to a higher recovery factor than the one by steam injection. The model presented can be used to upscale nanocatalytic *in-situ* upgrading for reservoir scales and to determine the effect of the principal variables involved, in particular reaction rates, thermal diffusivity, time, and size of matrix blocks. A future study will include considering temperature dependent properties and also incorporating oil recovery by gravity drainage.

Acknowledgments

We recognize the support by the Fondo Sectorial CONACYT-Secretaría de Energía-Hidrocarburos through Project 280170 conv 2016-3, Red de Conocimiento Cero Incidentes en la Red de Ductos de Mexico.

Nomenclature

Bo Oil formation volume factor (m^3/m^3)
 H Convective heat transfer coefficient ($W/m^2 K$)
 C_{1D} Lumping constant (m^3)

H Formation thickness (m)
 g Acceleration due to gravity (m/s^2)
 k Rock permeability (mD)
 k Thermal conductivity ($W/m K$)
 kg Global reaction constant (1/s)
 L_m Half of matrix block thickness (m)
 q Heat flux (W/m^2)
 q_D Dimensionless heat flux
 q_o Oil production (m^3/s)
 Q_o Cumulative oil production (m^3)
 Q_{oT} Cumulative oil production at maximum temperature (m^3)
 Q_{Do} Dimensionless cumulative oil production
 T Temperature ($^{\circ}C$)
 T_r Reservoir temperature (K)
 T_{reac} Reaction temperature (K)
 T_{VR} Vacuum residue temperature (K)
 T_D Dimensionless temperature
 T Time (s)
 t_{D1} Duration of the thermal penetration movement from the surface of matrix block to half of matrix block in dimensionless form
 t_{Dreac} Conversion/reactions time in dimensionless form
 t_{Dh} Cumulative time of hydroprocessing and initial heating up in dimensionless form
 t_{D2} Duration after reactions heating up in dimensionless form
 W Matrix block width (m)
 X Coordinate in Cartesian system
 Y Coordinate in Cartesian system
 α Thermal diffusivity (m^2/s)
 β Volumetric expansion coefficient (K^{-1})
 δ Heat penetration depth (m)
 ε Emissivity
 σ Stephen-Boltzmann coefficient (W/m^2K^4)
 Φ Rock porosity
 μ Viscosity

References

- Babadagli T. and Bahlani A. (2008). Heavy-oil recovery in naturally fractured reservoirs with varying wettability by steam solvent co-injection. October 20 - 23. Calgary, Alberta: *International Thermal Operations and Heavy Oil Symposium*. <https://doi.org/10.2118/117626-MS>.
- Babadagli T. (2003). Evaluation of EOR methods for heavy-oil recovery in naturally fractured reservoirs. *Journal of Petroleum Science and Engineering* 37, 25-37. [https://doi.org/10.1016/S0920-4105\(02\)00309-1](https://doi.org/10.1016/S0920-4105(02)00309-1)
- Coy Alejandro. (2013). *Experimental Simulation of a Hot Fluid Injection Process for In-reservoir Upgrading*. Master of Science Thesis, University of Calgary, Canada.
- Elahi S. M., Milad A., Scott C., Pereira A. (2018). *In-situ* upgrading of heavy oil using nanocatalysts: A computational fluid dynamic study of hydrogen and vacuum residue injection. *The Canadian Journal of Chemical Engineering* 58, 534-548. <https://doi.org/10.1002/cjce.23387>
- Ferno M. A. (2012). *Introduction to Enhanced Oil Recovery (EOR) Processes and Bioremediation of Oil-Contaminated Sites*. IntechOpen, Croatia.
- Galarraga Carmen Elena. (2011). *Upgrading Athabasca bitumen using NiWMo Catalyst at conditions near to in-reservoir operation*. Degree of Doctor of Philosophy Thesis, University of Calgary, Canada.
- Goodman T.R.(1964). Application of integral methods to transient nonlinear heat transfer. *Advances in Heat Transfer* 29, 51-122. [https://doi.org/10.1016/S0065-2717\(08\)70097-2](https://doi.org/10.1016/S0065-2717(08)70097-2)
- Haseli Y., van Oijen J.A. and de Goey L.P.H. (2012). Predicting the pyrolysis of single biomass particles based on a time and space. *Journal of Analytical and Applied Pyrolysis* 96, 126-138. <https://doi.org/10.1016/j.jaap.2012.03.014>
- Hassazadeh H., and Abedi J. (2010). Modelling and parameter estimation of ultra-dispersed in situ catalytic. *Fuel* 89, 2822-2828. <https://doi.org/10.1016/j.fuel.2010.02.012>
- Huirache-Acuña R., Sanchez-Bautista M. G., Lemus-Ruiz J., Ornelas C., Paraguay-Delgado F., and Rivera-Muñoz E. M. (2010). Synthesis and characterization of partially sulfide CoMoW oxides nanostructures and their application in the HDS and DBT. *Revista Mexicana de Ingeniería Química* 9, 209-218.
- Lashgari H., Delshad M., Sepehrnoori K., and Rouffignac E. (2016). Development and application of electrical-Joule-heating simulator for heavy oil reservoirs. *SPE Journal* 21, 215 - 228. <https://doi.org/10.2118/170173-PA>
- Martínez-Méndez E. J., Vázquez-Rodríguez R., Torijano-Cabrera E., and Hernpández-Escoto H. (2006). Small length scale analysis of the heat transport process in a semi-porous region of a geothermal well. *Revista Mexicana de Ingeniería Química* 5, 59-70.
- Mollaie A., Maini B., and Jalilavi M. (2007). Investigation of steam flooding in naturally fractured reservoirs. December 4-6. Dubai, U.A.E. *International Petroleum Technology Conference*. <https://doi.org/10.2523/IPTC-11087-MS>
- Nolan J.B., Ehrlich R., and Crookston R.B. (1980). *Applicability of Steamflooding for Carbonate Reservoirs*. April 20-23. Tulsa, U.S. SPE/DOE Symposium on EOR. <https://doi.org/10.2118/8821-MS>.
- Norasyikin I., Klock K., Hascakir B. (2016). *in-situ* Combustion Experience in Heavy Oil Carbonate. June 7-9. Calgary, Canada. *Canada Heavy Oil Technical Conference*. <https://doi.org/10.2118/180724-MS>
- Olea-Gonzalez U., Vazquez-Rodriguez A., García-Gutierrez A., and Anguiano-Rojas P. (2007). Estimation of formation temperatures in reservoirs: Inverse method. *Revista Mexicana de Ingeniería Química* 6, 65-74.
- Pereira-Almao P. (2012). *in-situ* upgrading of bitumen and heavy oils via nanocatalysis. *The Canadian Journal of Chemical Engineering* 31, 320-329. <https://doi.org/10.1002/cjce.21646>

Pooladi-Darvish M., Farouq-Ali S. M., and Tortike W. S. (1994). Non-Isothermal Gravity Drainage Under Conduction Heating. June 12-15. Calgary, Canada. *45th anual technical meeting of the Petroleum Society*. <https://doi.org/10.2118/94-65>

Rendon Vanesa. (2011). *In-Situ Upgrading by Continious Injection of Sub-micron Catalyst at Moderate Temperatures with Hydrogen Addition*. Master of Science Thesis, University of Calgary, Canada.

Sherratt J., Sharifi A., and Roozbeh R. (2018). Hot solvent-assisted gravity drainage in naturally fractured heavy oil reservoirs: A new model and approach to determine optimal solvent injection temperature. *American Chemical Society* 57, 3043-3058.

Souraki Y., Hassan K., and Ole T. (2011). Experimental Investigation and Numerical Simulation of Steam Flooding in Heavy Oil Fractured Reservoir. May 7-11. Anchorage, U.S. *SPE Western North American Region Meeting*.

van Heel A.P.G, Boerrighter P.M. and van Dorp J.(2008). Heavy-oil recovery by steam injection in fractured reservoirs. April 20-23. Tulsa, U.S. *Improved Oil Recovery Symposium*. <https://doi.org/10.2118/113461-MS>

van Wunnik J.N.M., and Wit K. (1992). Improvement of gravity drainage by steam injection into a fractured reservoir: An analytical evaluation. *SPE Journal* 7, 59-67.

Verlaan M., Boerrigter P.M. and van Dorp J. (2008). Experimental investigation of steam injection in light oil fractured carbonates. April 20-23. Tulsa, U.S. *Improved Oil Recovery Symposium*.

Appendix A: Derivation of the early-time regime

The Heat Integral Method (Goodman, 1964) considers a particular form of temperature distribution which depends on an unknown heat penetration depth. In this case a third order polynomial is chosen for the temperature profile $T_D(x_D, t_D)$ in the form of:

$$T_D = a(t_D) + b(t_D)x_D + c(t_D)x_D^2 + d(t_D)x_D^3 \quad (A.1)$$

The coefficients of the polynomial, which are functions of time, are found from the actual boundary conditions (Eq.10 and Eq.11) and two other auxiliary boundary conditions. The additional boundary conditions are defined using the properties of penetration depth.

1. For $x_d \geq \delta(t_d)$ the system is at equilibrium:

$$T_D(x_D = \delta_D, t_D) = 0 \quad (A.2)$$

2. There is no heat transferred beyond the penetration depth:

$$\frac{\partial T_D}{\partial x_D}(x_D = \delta_D, t_D) = 0 \quad (A.3)$$

The temperature distribution is obtained using the boundary conditions:

$$T_D = \left(1 - \frac{x_D}{\delta_D}\right)^3 \quad (A.4)$$

To obtain the expression of penetration depth we need to apply a space integration to Equation 8 from $x_D = 0$ to $x_D = \delta_D$. The result, which is Equation A.5, is referred as the heat-balance integral:

$$\frac{d}{dt_D} \int_0^{\delta} T_D dx_d = \frac{\partial T_D}{\partial x_D} \Big|_{\delta} - \frac{\partial T_D}{\partial x_D} \Big|_0 \quad (A.5)$$

Using Equation A.5 and the appropriate boundary conditions the penetration depth is obtained as:

$$\delta = \sqrt{24t_D} \quad (A.6)$$

Substituting the penetration depth into Equation A.4 the temperature profile can be written as:

$$T_D = \left(1 - \frac{x_D}{\sqrt{24t_D}}\right)^3 \quad (A.9)$$

Appendix B: Derivation of the pseudo-steady-state temperature

The hydroprocessing heating stage is represented by a third order polynomial temperature profile $T_D(x_D, t_D)$ as:

$$T_{Dh} = (t_D) + b(t_D)x_D + c(t_D)x_D^2 + d(t_D)x_D^3 \quad (B.1)$$

The time dependent coefficients of Equation B.1 are obtained through performing a space integration of Equation 8. Equations B.2 and B.3 show the results of the space integration:

$$\frac{d}{dt} \int_0^1 T_D dx_D = \frac{\partial T_D}{\partial x_D} \Big|_1 - \frac{\partial T_D}{\partial x_D} \Big|_0 \quad (\text{B.2})$$

$$\frac{d}{dt} \left[a(t_D) + \frac{b(t_D)}{2} + \frac{c(t_D)}{3} + \frac{d(t_D)}{4} \right] = 2c(t_D) + 3d(t_D) \quad (\text{B.3})$$

The coefficients that are functions of dimensionless time can be found by substituting the following boundary conditions:

$$\frac{\partial T_D}{\partial x_D} \Big|_{x_D=0} = q_D \quad (\text{B.4})$$

$$\frac{\partial T_D}{\partial x_D} \Big|_{x_D=1} = 0 \quad (\text{B.5})$$

$$T_D \left(x_D = 0, t_{D1} = \frac{1}{24} \right) = 1 \quad (\text{B.6})$$

$$T_D \left(x_D = 1, t_{D1} = \frac{1}{24} \right) = 0 \quad (\text{B.6})$$

Equations B.4 and B.5 are the actual boundary conditions, whereas Equations B.6 and B.7 are obtained by substituting the correspondent values of x_D and t_{D1} into Equation B.1. The temperature distribution is finally obtained as:

$$T_{Dh} = 1 + q_D \left(t_D - \frac{1}{24} \right) - q_D x_D + (2q_D - 3)x_D^2 + (2 - q_D)x_D^3 \quad (\text{B.7})$$

Appendix C: Derivation of the late-time solution

Following the procedure provided by (Pooladi-Darvish, et al., 1994), two temperature profiles were proposed:

$$T_{D1} = a(t_D) + b(t_D)x_D + c(t_D)x_D^2 \quad (\text{C.1})$$

$$T_{D2} = d(t_D) + e(t_D)x_D + f(t_D)x_D^2 \quad (\text{C.2})$$

Four of the six transient coefficients are solved by substituting the following boundary conditions:

$$T_{D1} = T_{Dh}(x_D = 0, t_d = t_{Dh}) = cte \quad (\text{C.3})$$

$$T_{D1} = T_{D2} \quad \text{at} \quad x_D = \frac{1}{2} \quad (\text{C.4})$$

$$\frac{\partial T_{D2}}{\partial x_D} \Big|_{x_D=1} = 0 \quad (\text{C.5})$$

$$\frac{\partial T_{D2}}{\partial x_D} \Big|_{x_D=1/2} = \frac{\partial T_{D1}}{\partial x_D} \Big|_{x_D=1/2} \quad (\text{C.6})$$

Substituting Equations C.3 to C.6 into Equations C.1-C.2 we can simplify the system of equations as:

$$T_{D1} = T_{Dh}(0, t_{Dh}) + b(t_D)x_D + c(t_D)x_D^2 \quad (\text{C.7})$$

$x_D \in [0, 1/2]$

$$T_{D2} = T_{Dh}(0, t_{Dh}) + b(t_D) \left(-\frac{1}{4} + 2x_D - x_D^2 \right) + c(t_D) \left(-\frac{1}{2} + 2x_D - x_D^2 \right) \quad (\text{C.8})$$

$x_D \in [0, 1]$

Integrating of Equation 4.8 from $x_D = 0$ to $x_D = \frac{1}{2}$ and $x_D = \frac{1}{2}$ to $x_D = 1$. Hence:

$$\frac{d}{dt} \int_0^{1/2} T_{D1} dx_D = \frac{\partial T_{D1}}{\partial x_D} \Big|_{1/2} - \frac{\partial T_{D1}}{\partial x_D} \Big|_0 \quad (\text{C.9})$$

$$\frac{d}{dt} \int_{1/2}^1 T_{D2} dx_D = \frac{\partial T_{D2}}{\partial x_D} \Big|_1 - \frac{\partial T_{D2}}{\partial x_D} \Big|_{1/2} \quad (\text{C.10})$$

Equations C.9 and C.10 are simplified by substituting Equations C.7 and C.8 into the appropriate equation. After simplifying two ordinary differential equations are obtained:

$$-b(t_D) - c(t_D) = \frac{1}{3} \frac{\partial b(t_D)}{\partial t_D} + \frac{5}{24} \frac{\partial c(t_D)}{\partial t_D} \quad (\text{C.11})$$

$$8c(t_D) = \frac{\partial b(t_D)}{\partial t_D} + \frac{1}{3} \frac{\partial c(t_D)}{\partial t_D} \quad (\text{C.12})$$

Simultaneously solving the above system we get:

$$c(t_D) = c_1 e^{-\frac{24}{7}t_D(3\sqrt{2}+5)} + c_2 e^{\frac{24}{7}t_D(3\sqrt{2}+5)} \quad (\text{C.13})$$

given by:

$$d(t_D) = c_1(-2 + \sqrt{2})e^{-\frac{24}{7}t_D}(3\sqrt{2}+5) + c_2(-2 + \sqrt{2})e^{\frac{24}{7}t_D}(3\sqrt{2}+5) \quad (C.14)$$

$$\left. \frac{\partial T_{D1}}{\partial x_D} \right| = -q_D \quad (C.15)$$

Finally two more boundary conditions should be used to find coefficients c_1 and c_2 . These conditions are

$$T_{D2} = q_d(t_{Dh} - \frac{1}{24}) \quad (C.16)$$

The coefficients c_1 and c_2 are obtained:

$$c_1 = \frac{1}{200} \frac{(-1482 + 550q_D + 1200q_D t_{Dh} - 741\sqrt{2} + 425\sqrt{2}q_D + 600\sqrt{2}q_D t_{Dh})\sqrt{2}}{e^{-\frac{72}{35}\sqrt{2} - \frac{24}{7}}} \quad (C.17)$$

$$c_2 = \frac{1}{200} \frac{(1482 - 550q_D + 1200q_D t_{Dh} - 741\sqrt{2} + 425\sqrt{2}q_D + 600\sqrt{2}q_D t_{Dh})\sqrt{2}}{e^{\frac{72}{35}\sqrt{2} - \frac{24}{7}}} \quad (C.18)$$